Optical Engineering 45(2), 023601 (February 2006)

Measurement of sectional profile of V-shaped metal cylinders using a sinusoidally vibrating interference pattern

Jinhuan Li, MEMBER SPIE
Niigata University
Graduate School of Science and Technology
Niigata-shi 950-2181, Japan
E-mail: Jinhuan_li@yahoo.com.cn

Osami Sasaki, MEMBER SPIE
Takamasa Suzuki, MEMBER SPIE
Niigata University
Faculty of Engineering
Niigata-shi 950-2181, Japan

Abstract. A method is proposed for accurately measuring a sectional profile of a metal cylinder. In this method a sinusoidally vibrating sinusoidal interference pattern is used to generate an exact spatial scale along one direction. Light from top points of a metal cylinder surface is extracted by spatial filtering in an afocal imaging system to form an image of the top points. A time-varying signal is detected in the image, and a sectional profile of the metal cylinder is measured from the phase of the detected signal on a position where the amplitude of the signal has a maximum value. Detection of the amplitude and the phase is carried out easily and exactly with sinusoidal phase-modulating interferometry.
 [DOI: 10.1117/1.2166848]

Subject terms: sectional profile measurement; interference pattern; sinusoidal phase-modulation; optical imaging.

Paper 040550RR received Aug. 12, 2004; revised manuscript received Apr. 11, 2005; accepted for publication Jun. 14, 2005; published online Feb. 3, 2006.

1 Introduction

It is important to measure shapes of screw-thread gauges with a short measuring time and high accuracy. Generally techniques based on mechanical probing of a thread using spherical or cylindrical probing elements are used for the shape measurement.[1] These techniques need a long measuring time and do not provide high accuracy. Noncontact optical probes using a triangulation method or a confocal method are being considered for improvement of the measurement accuracy. These optical probes, however, are not suitable for measuring a sectional profile of the thread gauge, because the sloping part of the thread is far from perpendicular to the probing direction of the optical probe.

In another optical technique, collimated light is incident on the thread gauge, and a magnified image of its sectional profile is formed with the light passing the edge of thread gauge. The image is detected with a two-dimensional CCD image sensor. Since the positions of the edge of the thread gauge in the image are decided by using the pixel positions of the CCD image sensor, the measurement accuracy and the measurement region depend on the pixel size and number of pixels. When the measurement region is small, the thread gauge must be mechanically moved up and down to measure the section profiles on both the upper and lower sides. This movement degrades the measurement accuracy and lengthens the measuring time.

In order to extend the measurement region, we use a sinusoidally vibrating interference pattern (SVIP) with period P as an exact spatial scale along one direction, the x axis.[2,3] Although our final aim is to measure shapes of thread gauges by using the SVIP, a metal cylinder with a V-shaped groove was used as an object in the initial trials. This simple object makes it easy to examine characteristics of the application of the SVIP to the measurement of a sectional profile of a metal cylinder.

The SVIP is projected on the metal cylinder surface. The light from the top points of the cylinder surface is extracted by spatial-frequency filtering in an optical system so that the images of the top points are formed. On the image plane a time-varying signal owing to the SVIP is detected with a two-dimensional CCD image sensor. A value of the x coordinate of a top point on the surface is obtained from the phase of the detected signal at the position where the amplitude of the signal is a maximum along the x axis. The phase measurement accuracy can be easily made about $P/200$ by using sinusoidal phase-modulating interferometry. An average phase is detected over one pixel of the CCD image sensor if a side of the pixel is smaller than about $P/8$. From these characteristics of phase detection a wide measurement region and high measurement accuracy can be obtained in the method proposed in this paper.

2 Instrument

The configuration of an instrument for measuring a sectional profile of a metal cylinder is shown in Fig. 1. The

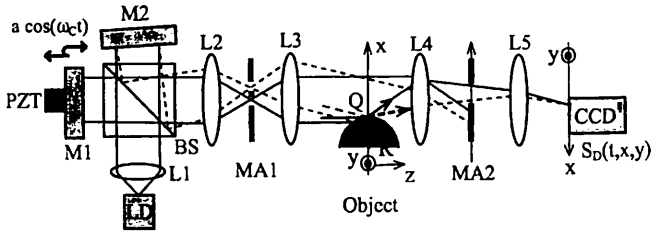

Fig. 1 Configuration of an instrument for measuring sectional profiles of metal cylinders.

0091-3286/2006/$22.00

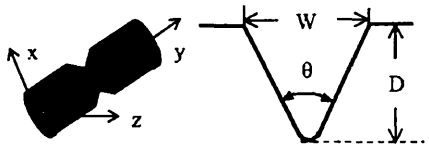

Fig. 2 Metal cylinder and its V-shaped groove.

output light beam from a laser diode (LD) is collimated by the lens L1 and divided into two beams by a beamsplitter (BS). The two beams are reflected by two mirrors M1 and M2, respectively. The reflected beams from M1 and M2 pass through the beamsplitter and are combined again. By adjusting the inclinations of M1 and/or M2, an interference fringe pattern of period P parallel to the y axis is obtained. The collimated laser beams forming the interference pattern enter the afocal imaging system, which consists of lenses L2 and L3. On the spectral plane of this imaging system, the mask MA1 with two pinholes eliminates undesirable light for the formation of the interference pattern. The interference pattern, with an exact sinusoidal intensity distribution, is obtained and projected on the surface of an object. The object is a metal cylinder whose diameter changes along the y axis according to the sectional profile, as shown in Fig. 2. A top point of the sectional profile is denoted by Q as shown in Fig. 1. Assuming that the intensities of the two beams and the visibility of the fringes are unity for the sake of simplicity, the sinusoidal intensity distribution on the x-y plane where an object is placed is expressed by

$$I(x,y) = 1 + \cos\left(\frac{2\pi}{P}x\right). \tag{1}$$

When the mirror M1 is vibrated by a piezoelectric transducer (PZT) with a sinusoidal waveform $a\cos(\omega_c t)$, the interference pattern is vibrated sinusoidally along the x axis. This sinusoidally vibrating interference pattern (SVIP) is expressed by

$$I(t,x,y) = 1 + \cos\left[Z\cos(\omega_C t) + \frac{2\pi}{P}x\right], \tag{2}$$

where

$$Z = \frac{2\pi}{P}a. \tag{3}$$

The surface of the metal cylinder diffracts and reflects the two beams, forming the SVIP. An afocal imaging system, which consists of lenses L4 and L5, is used to form an image of the sectional profile. A mask MA2 is put in the spectral plane of the afocal imaging system to select the light coming from the top points of the object surface. The intensity distribution in the image plane is expressed by

$$I_D(t,x,y) = A(x,y) + B(x,y)\cos[Z\cos(\omega_C t) + \alpha(x,y)], \tag{4}$$

where $A(x,y)$, $B(x,y)$, and $\alpha(x,y)$ depend on the sectional profile of the object and a shape of the mask MA2.

The intensity distribution $I_D(t,x,y)$ is the same as the interference signal produced in a sinusoidal phase-modulating (SPM) interferometer.[4] The method for detecting the interference signal with a two-dimensional CCD image sensor using a shutter function was reported in Ref. 5. We use the same method to detect the intensity distribution $I_D(t,x,y)$ with a CCD image sensor. The time-varying component of $I_D(t,x,y)$ is written as

$$S_D(t,x,y) = B(x,y)\cos[Z\cos(\omega_C t) + \alpha(x,y)]. \tag{5}$$

This signal $S_D(t,x,y)$ detected with the CCD image sensor is processed in a computer by the method of SPM interferometry [4,6] to obtain $B(x,y)$ and $\alpha(x,y)$.

In the next section, experimental results are given that show that the detection of the amplitude $B(x,y)$ and the phase $\alpha(x,y)$ leads to the measurement of a sectional profile of the object.

3 Experiments

3.1 *Experimental Setup*

Experiments were carried out with the instrument shown in Fig. 1. The power of the laser diode (LD) was 30 mW. The wavelength λ of the LD was 660 nm. The period P of the interference pattern was 100 μm. Lenses L2 and L3 had a same focal length of 100 mm. The diameter of the pinhole used in mask MA1 was 200 μm. The sinusoidal vibrating frequency $\omega_c/2\pi$ was 177 Hz. The diameter of the metal cylinder was 10 mm, and the V-shaped groove in its profile had width W, depth D, and angle θ equal to 1 mm, 1 mm, and 60 deg, respectively, as shown in Fig. 2. The focal lengths of the lenses L4 and L5 were 70 and 35 mm, respectively. The magnification of the afocal imaging system was $M = 1/2$, and the square region of one measurement point was 9.3×9.3 μm on the object.

3.2 *Experimental Result*

When the SVIP was projected onto the surface of the metal cylinder, we observed the intensity distribution on the spectral plane of the afocal imaging system with lenses L4 and L5, as shown in Fig. 3(a). This intensity distribution is the spectrum of the light diffracted and reflected from the different parts of the sectional profile of the metal cylinder, which is shown in Fig. 3(b). The two black circles in the lower part of Fig. 3(a) are pieces of black paper, which blocked the beams of strong intensity whose original propagation directions were not changed by the object. The parts of the sectional profile that are parallel to the y axis and denoted by A in Fig. 3(b) produced the beams that extended in the vertical direction from the black circles. These beams are denoted by A1 and A2 in Fig. 3(a), according to the numbering of the two collimated beams from which they originate. The left sloping part of the sectional profile, denoted by B_L produced the beams that extended diagonally upward to the right and are denoted by B_L1 and B_L2 in Fig. 3(a). The right sloping part of the sectional profile, denoted by B_R, produced the beams denoted by B_R1 and B_R2 in Fig. 3(a). In order to obtain only the light coming from the top points of the sectional profile of the object, we examined what kind of shape was the best for the mask MA2 as described later in this section. The beams selected by MA2 were used to form an image of the sectional profile of the metal cylinder along the y axis.

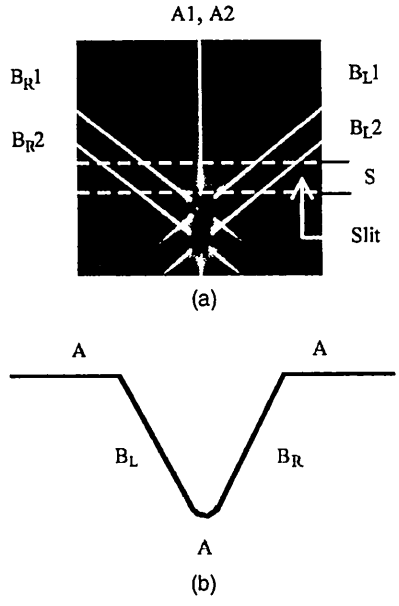

Fig. 3 (a) Intensity distribution on the spectrum plane, and (b) part of the V-shaped sectional profile.

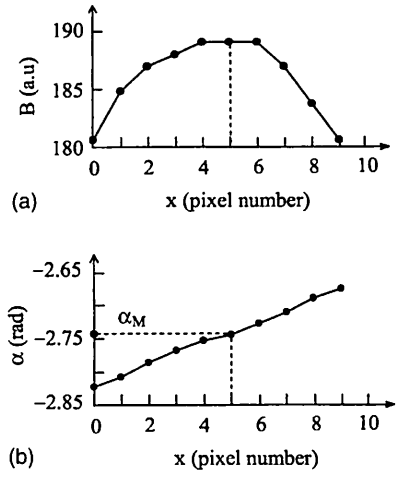

Fig. 5 Distribution of (a) amplitude B and (b) phase α detected along x axis at a fixed value of the y coordinate.

The light intensity distribution of the image is shown in Fig. 4. This picture was taken while the mirror M1 did not vibrate. When M1 was vibrated, the time-varying light intensity $I_D(t,x,y)$ was detected with the CCD image sensor. The amplitude $B(x,y)$ and the phase $\alpha(x,y)$ of $S_D(t,x,y)$ were calculated along the x axis at each y coordinate. Figure 5 shows the distribution $B(x,y)$ and the distribution $\alpha(x,y)$ calculated at a y coordinate corresponding to the part B_L of the sectional profile. The distribution $B(x,y)$ has one peak, and the phase $\alpha(x,y)$ varies very slightly along the x axis. The sectional profile of the metal cylinder is provided by the phase value $\alpha_M(y)$ that was detected at the peak of the amplitude distribution $B(x,y)$, as shown in Fig. 5. The sectional profile is calculated with

$$r(y) = P\alpha_M(y)/2\pi. \tag{6}$$

When there is uncertainty in determining the position of the maximum value of the amplitude $B(x,y)$, this uncertainty causes a measurement error. A smaller phase difference between adjacent measurement points, leads to a smaller error. In addition, a smaller phase difference leads to a larger interval between measurement points or a larger measurement region. Therefore, it is very important to be able to decrease the phase difference. The mask MA2 was the dominant factor in doing so. The shape, width, and position of MA2 were decided as described below.

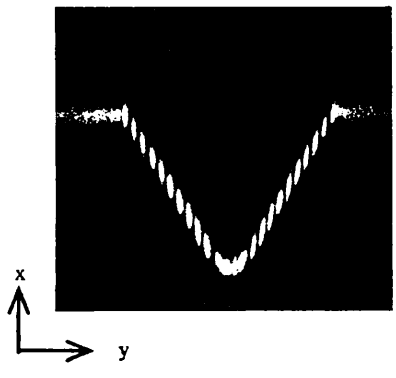

Fig. 4 Image of the sectional profile on the detecting plane.

First, in order to examine the shape of MA2 suitable for selecting parts of beams B_L1 and B_L2 whose lengths were equal, we used a rectangular slit. We changed the angle of the slit relative to the beams A1 and A2. When the slit was perpendicular to A1 and A2, the phase difference $\alpha(x,y)$ between adjacent measurement points was smallest. Because B_L1, B_L2, B_R1, and B_R2 were symmetric with respect to A1 and A2, the most suitable slit for B_R1 and B_R2 was the same as for B_L1 and B_L2. From this result a straight slit, shown in Fig. 3(a) with dashed lines, was chosen as the best and simplest.

Next, it is desired that the light coming from the top-points of the sectional profile be selected by a rectangular slit of very small width. However, when the width of the slit was too narrow, the intensity of the image was too weak for the CCD image sensor. For this reason the width S of MA2 employed was 300 μm.

Finally, it was observed that the phase difference between adjacent measurement points became larger when the slit MA2 was moved away from the two black circles shown in Fig. 3(a). This means that MA2 must be as close as possible to one of the black circles.

The finally determined slit of S=300 μm is shown in Fig. 3(a), and the difference of adjacent measurement points was about 0.02 rad, as shown in Fig. 5.

Figure 6 shows a measured sectional profile of the metal cylinder in which the width W, depth D, and angle θ of the V-shaped profile are indicated. The least-squares approximated lines of the measured profile were calculated to obtain the value of θ. We measured the sectional profile three times to examine the measurement repeatability. The measured values are shown in Table 1. They agreed with the values measured with an industrial microscope. The repeatability was about 0.5 μm in width W, 1 μm in depth D, and 0.01 deg in angle θ.

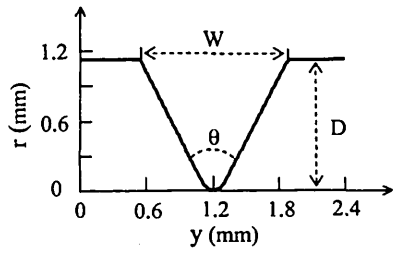

Fig. 6 Measured sectional profile of the metal cylinder. Measured values were W=1.317 mm, D=1.047 mm, and θ=60.01 deg.

4 Accuracy of Detected Phase α_M

The coordinates x and y of a top point of the metal cylinder are decided by the phase $\alpha_M(y)$ and the position of the CCD pixel along the y axis, respectively. The sectional profile of the metal cylinder contains a sloping part whose angle is 30 deg with respect to the x axis, as shown in Fig. 4. It should be considered how the phase $\alpha_M(y)$ is detected in the sloping part. We made a numerical analysis of the amplitude $B(x,y)$ and the phase $\alpha(x,y)$ of the signal detected with the two-dimensional CCD image sensor. We assumed that the light on the image plane comes from only the top points of the metal cylinder. On this assumption, the amplitude $B(x,y)$ is unity on the lines that represent the sectional profile of the metal cylinder. The phase $\alpha(x,y)$ is the phase of the interference pattern on the sectional profile. In the actual imaging, we used the slit MA2 of 300-μm width, which was put parallel to the y axis. This slit spreads the light along the x axis. The function expressing how the light is spread is the Fourier transform of the shape of the slit.

For the numerical analysis we selected five pixels along the y axis as shown in Fig. 7. The grid of thin solid lines represents the pixels of the CCD image sensor. A square region surrounding one measurement point was 9.3 $\times$9.3 μm on the object. The numbers i from 1 to 5 along the y axis expresses the position of the pixel on the CCD. The numbers from 0 to 9 along the x axis are the pixel numbers corresponding to the x coordinate. The thick solid line intersecting the x axis at an angle of 30 deg is the image of the sloping part of the sectional profile according to the assumption in the preceding paragraph. The optical field of amplitude B and phase α on the thick solid line is directed along the x-axis, and the sum of the fields incident on the pixel is detected with the CCD image sensor. The maximum amplitude along the x axis appears on the pixels shaded gray. Therefore it is expected that the phase $\alpha_M(i)$ will be equal to the phase α_i on the gray pixel at position i,

Table 1 Measured values.

Trial	W (mm)	D (mm)	θ (deg)
1	1.3173	1.047	60.01
2	1.3165	1.046	60.00
3	1.3169	1.046	60.00

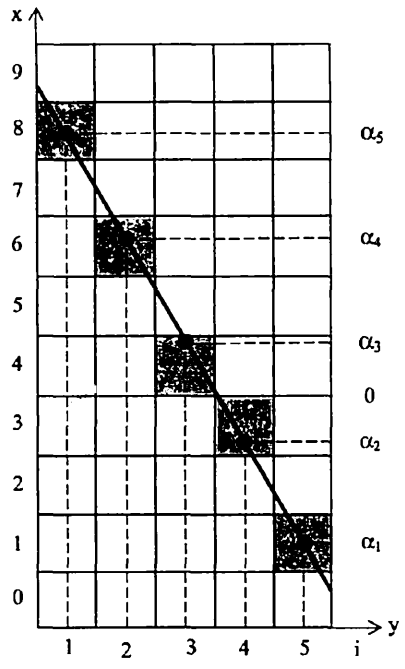

Fig. 7 Simulation model of optical field on the CCD image sensor.

where α_i is the phase at the midpoint of the pixel with respect to the y axis. These midpoints are indicated by black circles, and the phases α_i are indicated along the x axis. The phase α changes by 2π when the coordinate of the x axis changes by 100 μm. The phase α at the boundary between pixel 3 and pixel 4 along the x axis was assumed to be zero. We calculated the fields arising from the field on the thick solid line by spreading, and summed the spread fields over the pixel to obtain the values of $B(x,y)$ and $\alpha(x,y)$.

When the field at a position spreads along the x axis to positions separated by the pixel size of 9.3 μm, the amplitude attenuation of the spread field is just 0.98 for the 300-μm-width slit MA2. The results for position i=3 are shown in Fig. 8. The maximum amplitude along the x axis appears at pixel number 4, and the phase $\alpha_M(3)=\alpha_{M3}$ was

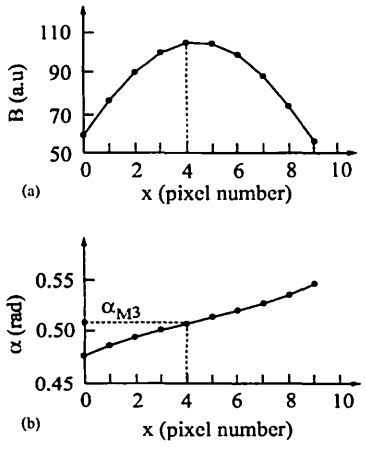

Fig. 8 Results of the simulation for (a) the amplitude B and (b) the phase α along the x axis at a fixed value of the y coordinate.

Table 2 Calculated values α_i compared with measured values α_{Mi}.

Position i	α_i (rad)	α_{Mi} (rad)	ε_α (rad)
1	−1.517	−1.520	0.003
2	−0.506	−0.509	0.003
3	0.506	0.503	0.003
4	1.517	1.515	0.002
5	2.530	2.527	0.003

0.503 rad. The amplitude and the phase distributions of Fig. 8 are similar to those of Fig. 5. All of the phases $\alpha_M(i)$ were calculated and compared with α_i as shown in Table 2, where $\varepsilon_\alpha = \alpha_i - \alpha_M(i)$. These results clearly show that the output of the CCD image sensor provides the phase of the sectional profile at the midpoint of the pixel along the y axis. When the pixel size was changed to 18.6×18.6 μm to obtain a larger measurement region, the error ε_α became 0.02 rad.

Considering that the error ε_α must be less than 0.02 rad, the required measurement range regarding the width, depth, and angle of the V-shaped profile can be determined. The maximum pixel size of 18.6×18.6 μm on the object determines a maximum size of the V-shaped profile with angle 60 deg, depending on the pixel number of the CCD image sensor. As the angle of the V-shaped profile becomes smaller, the maximum pixel size is reduced. At the same time, the slit MA2 must be changed so that the light coming from the sloping parts of the V-shaped profile is directed near the two black circles shown in Fig. 3.

5 Conclusion

A method for accurately measuring a sectional profile of a cylinder has been proposed. In this method an SVIP with a period of 100 μm was used to generate the exact spatial scale along the x axis. The light from the top point of the metal cylinder surface was extracted by spatial filtering in the afocal imaging system so that an image of the top point was formed. The sinusoidally phase-modulated signal was detected in the image. Detection of the amplitude and the phase of the signal was carried out easily and exactly by using sinusoidally phase-modulating interferometry. The sectional profile of the metal cylinder was obtained from the phase of the signal detected at the position where the amplitude of the signal was a maximum in the image. A V-shaped sectional profile of a metal cylinder was measured with a repeatability of about 0.5 μm in width W, 1 μm in depth D, and 0.01 deg in angle θ. The numerical results about the amplitude and the phase distributions of the signal agree with the experimental results. The conclusions given in this paper will be very useful in the next stage for measuring consecutive V-shaped structures or sectional profiles of screw-thread gauges.

References

1. European Co-operation for Accreditation (EA), "Determination of pitch diameter of parallel thread gauges by mechanical probing," EA publication EA-10/10, APR 1999, http://www.european-accreditation.org/.
2. O. Sasaki, K. Hashimoto, Y. Fujimori, and T. Suzuki, "Measurement of cylinder diameter by using sinusoidally vibrating sinusoidal gratings," *Proc. SPIE* **4416**, 34–38 (2001).
3. J. Li, O. Sasaki, and T. Suzuki, "Measurement of sectional profile of a cylinder using a sinusoidally vibrating light with sinusoidal intensity," *Opt. Rev.* **9**, 159–162 (2002).
4. O. Sasaki, Y. Ikeda, and T. Suzuki, "Superluminescent diode interferometer using sinusoidal phase modulation for step-profile measurement," *Appl. Opt.* **37**, 5126–5131 (1998).
5. T. Suzuki, T. Maki, X. Zhao, and O. Sasaki, "Disturbance-free high-speed sinusoidal phase-modulating laser diode interferometer," *Appl. Opt.* **41**, 1949–1953 (2002).
6. O. Sasaki and H. Okazaki, "Sinusoidal phase modulating interferometry for surface profile measurement," *Appl. Opt.* **25**, 3137–3140 (1986).

Biographies and photographs of authors not available.